Analytica Chimica Acta 1166 (2021) 338579

Contents lists available at ScienceDirect

Analytica Chimica Acta

journal homepage: www.elsevier.com/locate/aca

Dual-signaling amplification strategy for glutathione sensing by using single gold nanoelectrodes

Hao Wang , Hongmei Hua , Haoran Tang , Yongxin Li *

Anhui Key Laboratory of Chemo/Biosensing, College of Chemistry and Materials Science, Anhui Normal University, Wuhu, 241000, PR China

HIGHLIGHTS

- Dual-signaling Amplification Strategy for Glutathione Sensing with high sensitivity and selectivity was developed.
- The nanosensor was fabricated on single gold nanoelectrodes developed by laser-assisted pulling technique.
- This developed nanosensor with small overall dimension can be used for single cell/organelle analysis.

GRAPHICAL ABSTRACT

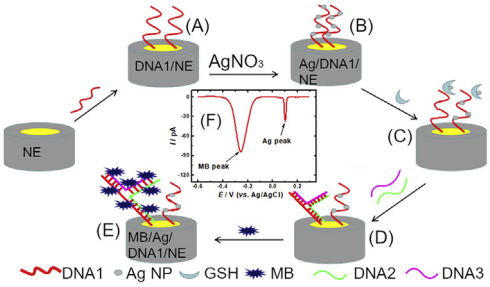

ARTICLE INFO

Article history:
Received 20 January 2021
Received in revised form
5 April 2021
Accepted 23 April 2021
Available online 30 April 2021

Keywords:
Nanoelectrode
Dual-signaling ratiometric sensors
Methylene blue
Electrochemical biosensor
Glutathione

ABSTRACT

A new nanosensor for glutathione (GSH) detection by use of single nanoelectrodes has been developed through a dual-signaling ratiometric amplification strategy. Ag nanoparticles (Ag NPs) metalized DNA1 was modified on an Au nanoelectrode surface. Due to the strong affinity between Ag NP and GSH, Ag NPs could be removed by the addition of GSH. The remaining metalized DNA1 could hardly form a double strand, while the de-metalized DNA1 could hybrid with DNA2 and DNA3 to form a complex structure to adsorb methylene blue (MB), and then the electrochemical signal of differential pulse voltammetry (DPV) from MB oxidation could be observed. With the addition of GSH, the peak current of MB oxidation at about −0.27 V (I_{MB}) increases, while the signal of Ag oxidation at about 0.1 V (I_{Ag}) decreases. It was found that there had a linear relationship between the ratio of dual-signal (I_{MB}/I_{Ag}) and the GSH concentrations, which could be used to detect GSH. The ratiometric nanosensor is label-free, easy to operate, and can eliminate inherent system errors. Considering the advantages of nanoelectrodes, such as low *IR* drop, fast response, and small overall dimension, this developed nanosensor can be used for GSH detection living systems (e.g., cell lysate).

1. Introduction

Glutathione (GSH) is a naturally active non-protein thiol species that play a key role in the free radical biological systems [1], and the maintenance of appropriate biological functions in organisms [2]. As an important tripeptide thiol (γ-glutamyl cysteinyl glycine) antioxidant, it widely exists in human cells with a high concentration (1–10 mM) [3,4]. The concentration changes of the GSH is directly related to the occurrence of some diseases, such as neurodegenerative disorders, inflammation, heart disease, and cancer, etc. [5,6] Therefore, the measurement and quantification of GSH holds promising biological and clinical significance and has become the important research subject, which gains great concerns

* Corresponding author.
E-mail address: yongli@mail.ahnu.edu.cn (Y. Li).

https://doi.org/10.1016/j.aca.2021.338579
0003-2670/

of the researchers [7,8].

Many strategies have been developed for the detection of GSH [9–18], however, these methods all focus on in-vitro testing, and cannot be used for in-vivo detection. Nanoelectrodes (NEs) are a type of electrodes with a diameter of less than 100 nm, which have attracted wide interest because of their high mass-transport rate, lower RC constant, smaller overall dimension, and the reduced effect of solution resistance [19–24]. Due to their small size, NEs are expected as a useful platform to fabricate a new type of intracellular electrochemical sensor.

NEs-based sensors have been studied by many researchers because they have the potential to record with a high spatiotemporal resolution, but have minimal interference with cell function [25,26]. For example, Jena and Zhang et al. [27] and Salamifar and Lai et al. [28] adopting the electrodeposition method to fabricated Au nanodisk-electrodes to ferrocene counting and DNA sensing. Schuhmann's group [26,29] and Mirkin's group [30,31] introduced Prussian blue/Pt modified nanoelectrodes into in-vivo detection of reactive oxygen and nitrogen species. We also developed nanosensors based on gold nanoelectrodes for bioanalysis [32–34]. However, NEs-based sensors have their shortages such as low sensitivity due to their limited electroactive area, it is still necessary to explore the novel approaches with high sensitivity and selectivity.

Herein, we have designed a dual-signal ratiometric amplification strategy based on gold nanoelectrodes for GSH detection by DNA metallization using Ag nanoparticles and methylene blue (MB) as signals. Our strategy is illustrated in Scheme 1. Thiol-modified DNA1 was firstly modified on a gold NE (**A**). After that, the conjugated DNA1 was adopted as the platform for adsorbing AgNPs, which would hinder further DNA hybridization by disturbing DNA base pairing (**B**). Because of the stronger interaction between GSH and AgNPs, when the GSH was added to the system, the AgNPs could be detached from DNA1 (**C**), resulting in a significant decrease of the current of Ag oxidation peak (shown in **F**, peaks at ~0.1V). The released DNA1 further hybridized with DNA2 and DNA3 to form long DNA fragments (**D**). Finally, methylene blue (MB) was introduced to the system (**E**). The prepared sensor was then measured the oxidation current of MB and Ag (I_{MB} at ~ -0.27 V and I_{Ag} at ~0.1 V, shown in **E** and **F**) by differential pulse voltammetry (DPV). With the addition of GSH, the current of MB oxidation at about −0.27 V (I_{MB}) increases, while the signal of Ag oxidation at about 0.1 V (I_{Ag}) decreases. A linear relationship between the quotient of current changes (I_{MB}/I_{Ag}) and the GSH concentrations could be obtained, which can be used to detect GSH. The proposed assay is label-free and easy to operate, avoiding the use of dye-modified sensors. Most significantly, a ratiometric nanosensor can eliminate inherent system errors. These unprecedented advantages make the determination highly sensitive and accurate. Considering the advantages of nanoelectrodes, such as low *IR* drop, small overall dimension, and fast response, this developed nanosensor can be used for GSH detection in living systems (e.g., cell lysate).

2. Experimental section

2.1. Materials and reagents

Ferrocene (Fc, Fluka); tetra-n-butylammonium hexafluorophosphate ($TBAPE_6$, Aldrich); acetonitrile (ACN, Shanghai Chemical Co. Shanghai, China); 4-(2-hydroxyethyl)-1-piperazineethanesulfonic acid (HEPES, Aldrich); mercaptohexanol (MCH), silver nitrate ($AgNO_3$), sodium borohydride ($NaBH_4$), Tris, EDTA, HCl, NaCl, $NaNO_3$, H_2SO_4, ethanol (CH_3CH_2OH), methylene blue (MB) purchased from Shanghai Reagent Company; phosphate buffer saline (PBS) solution (Shanghai Lingfeng Chemical Reagent Co., Ltd.); glutathione (GSH), L-cysteine (Cys), glutamine (Gln), threonine (Thr), tryptophan (Trp), glycine (Gly) purchased from Shanghai Reagent Company; double distilled water (DDW, Milli-Q, Millipore Co.) All reagents were of analytical purity without further purification.

Au microwires (diameter = 25 μm) and Tungsten wires (diameter = 250 μm) were obtained from Alfa Aesar. Glass capillaries (inner diameter = 0.64 mm, outer diameter = 1.0 mm) were ordered from Sutter Instrument Co. The NEs were polished with different finer grit sandpapers (1200, 600, and 200 grits) and Al_2O_3 powders (1.0, 0.3, and 0.05 μm) before experiments.

Different DNAs were purchased from Sangon Biotech Co., Ltd. (Shanghai, China), and their solution in 10 mM Tris-HCl (pH = 7.4) was stored at 4 °C. HeLa cells were obtained from the local cell culture center. All of the DNA sequences were shown in supporting information (Table S1).

2.2. Apparatus

All of the NEs were fabricated by our previously reported method by employing a P-2000 laser-assisted puller (Sutter Company, IL, USA) [35]. An optical microscope (OLYMPUS BX53, Japan) was adopted to observe the continuity of the tips of NEs. Scanning electron microscope (SEM) images were captured by an S-4800 scanning electron microanalyzer (Hitachi, Japan). All experiments were carried out with a three-electrode system using an electrochemical workstation (CHI 660D, Chenhua Instruments Co. Ltd., Shanghai, China) at room temperature. An Ag/AgCl electrode was used as the reference electrode and a Pt wire was used as a counter electrode. All of the TEM images were taken from Tecnai G2 (Fei, USA).

2.3. Preparation of the nanosensor

Gold nanoelectrodes were first polished to obtain different radius nano-disk nanoelectrodes with different fine-grit sandpapers and different particle sizes alumina slurries. Because the radius depends on hand-grinding process, the size of the electrode will have an error of about 1 nm. The radius of the NEs was calculated by the limiting steady-state current (See **Characterization of the gold nano-disk electrodes** section and Supporting Information, Fig. S1 for more information). Nanoelectrodes with a radius of about 54–55 nm were used in this experiment. The prepared NEs were then immersed in 0.5 M H_2SO_4 solution for electrochemical pretreating. The NEs were finally washed with ultra-pure water and then dried under a nitrogen atmosphere.

The NEs were immersed in a 1.0×10^{-6} M DNA1 solution at 37 °C for 6 h to prepare the DNA1/NEs (Scheme 1A). The DNA1/NEs were then placed in a 1 mM mercaptohexanol (MCH) solution for 15 min to block the unreacted sites. To modify Ag nanoparticles, the DNA1/NEs were immersed in a HEPES buffer solution (pH = 7.4) containing 1 mM $AgNO_3$ for 1 h. Finally, the prepared electrodes were placed in a freshly prepared $NaBH_4$ solution (0.01 M in HEPES buffer) for 10 min to obtain Ag/DNA1/NEs (Scheme 1B).

2.4. Electrochemical detection of GSH

The detection mechanism was shown in Scheme 1. To detect GSH, the prepared Ag/DNA1/NEs were immersed in different concentrations of GSH solution for 1 h (Scheme 1C). After that, the nanoelectrodes were washed by PBS buffer and then immersed in a 1.0×10^{-6} M DNA2 and DNA3 solution at 37 °C for 2 h (Scheme 1D). Finally, the prepared electrode was immersed in 50 μM MB solution for 20min, followed by being washed with PBS. The MB modified nanoelectrode was signed as MB/Ag/DNA1/NEs (Scheme 1E), which was scanned at a potential range of −0.6 to 0.3 V versus Ag/AgCl

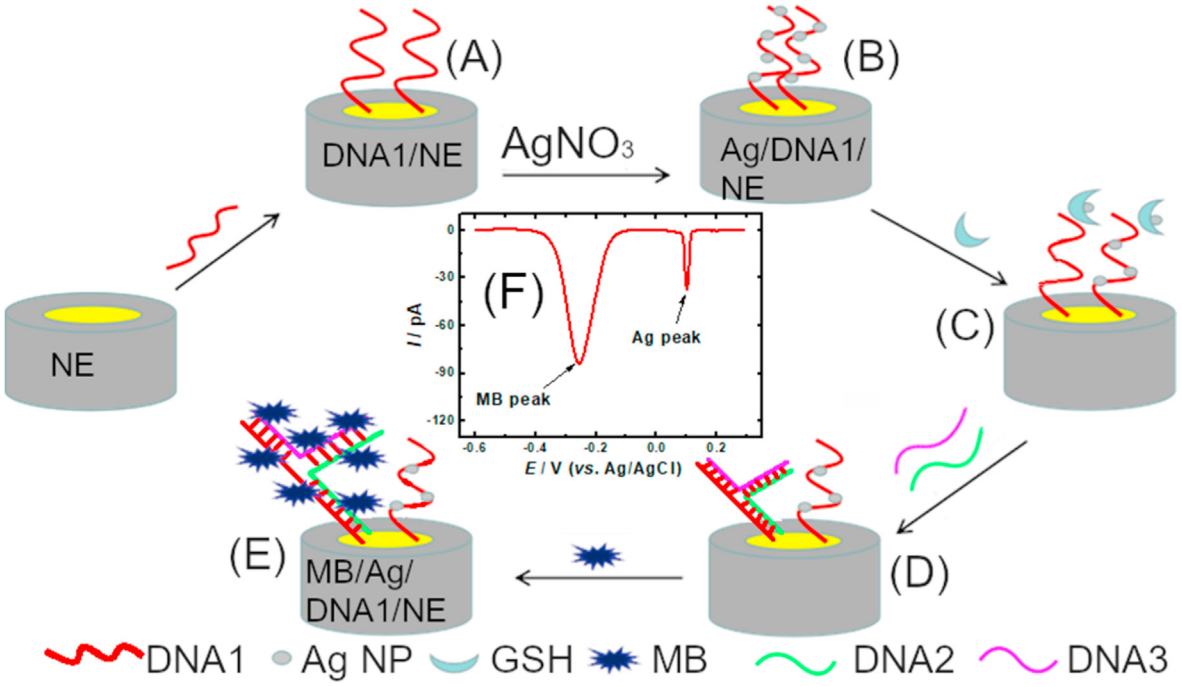

Scheme 1. Schematic diagram of GSH detection by construction dual-signaling ratiometric amplification sensors using gold nanodisk electrodes.

reference electrode by DPV in a 0.1 M NaCl and 0.1 M $NaNO_3$ mixture solution (Scheme 1F). The current ratio of MB peak to Ag peak in DPV was used as the signal to detect GSH ($I = I_{MB}/I_{Ag}$).

2.5. Detection of GSH levels in cell lysate

HeLa cells were cultured by our previously reported method [36]. The HeLa cells (1×10^6) were firstly washed with PBS twice, and then centrifuged and stored at 4 °C. To destroy the cells, 10 μL of 10 mM HCl was added. The mixture was then frozen in liquid nitrogen and dissolved in 37 °C water bath twice. After that, the cell solution was mixed with 20 μL of 5% sulfosalicylic acid solution and centrifuged to the collected supernatant. To measure the intracellular GSH levels, the cell lysate was further diluted 800-fold before use.

3. Results and discussion

3.1. Characterization of the gold nano-disk electrodes

The electrochemical behaviors of NEs with different radius were investigated with 5 mM Fc solution. The results were listed in Fig. S1A. The ideal sigmoidal shape could be observed in each curve and no obvious hysteresis on the reverse scan, indicating the NEs were fabricated very well. As Bard pointed out that the steady-state limiting current at disk-like NEs can be calculated using the following Eq. (1) [37].

$$i_d = 4nFDC_ba \quad (1)$$

Where i_d is the steady-state limiting current, n is the number of electrons transferred per molecule (1 in this case), D is the diffusion

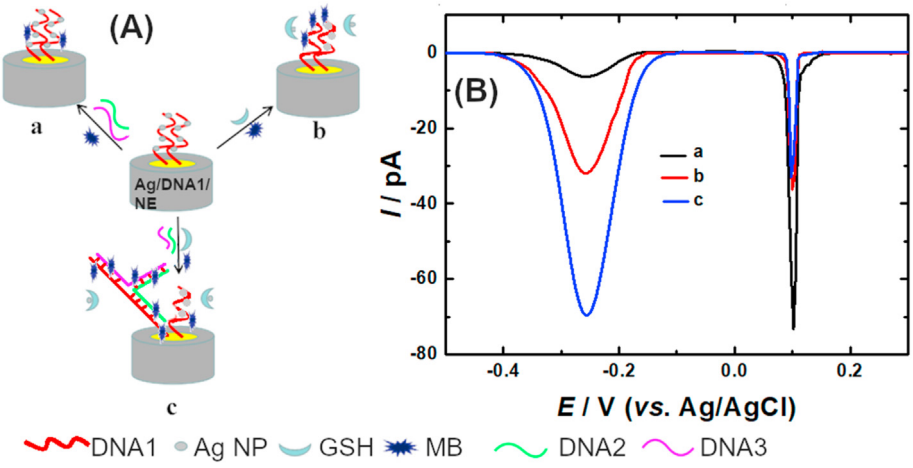

Fig. 1. (A) Schematic diagrama of the different modified electrodes: (a) MB + DNA2 + DNA3 + Ag/DNA1/NE, (b) MB + GSH + Ag/DNA1/NE, (c) MB + GSH + DNA2 + DNA3 + Ag/DNA1/NE; **(B)** DPV curves of the different modified electrodes, the diameter of Au nanodisk electrode was about 110 nm.

coefficient (for Fc, the value is 2.4×10^{-9} m^2/s), F is Faraday's constant, C_b is the concentration of Fc (5 mM), and a is the radius of NE. To directly prove the formation of gold nanoelectrodes, the SEM image of an NE with a radius of ~54 nm was obtained (Fig. S1B). Meanwhile, the COMSOL simulation data were shown in Fig. S1C, where the red curves were the CVs obtained by experiment and the black curves represent the COMSOL simulation. The two curves are fitted very well, indicating that the radii of NEs obtained by the electrochemical method were trustworthy.

3.2. Feasibility of the electrochemical biosensor

To evaluate the feasibility of the prepared dual-signaling sensor, three different modified electrodes were investigated (Fig. 1A). The DPV responses were shown in Fig. 1B. The peak at −0.27 V was the signal of MB, and the peak at about 0.1 V was the Ag oxidation peak. It should be noticed that the signal intensity of MB and Ag are different on three modified electrodes. As shown in Fig. 1A a, due to the metalized DNA cannot hybridization, the complex DNA structure cannot be formed, resulting in only a few amounts of MB attachment. It could be easily observed that the peak of silver oxidation in **curve a** (Fig. 1B) is much higher than the MB signal, indicating that only a few amounts of MB were attached to the sensors. When the GSH was introduced in this system, the current of Ag oxidation was significantly decreased due to the strong affiant binding between GSH and Ag (Fig. 1A b and Fig. 1B, **curve b**). At the same time, the MB signal in **curve b** was much higher than it in **curve a**, indicating that the MB could attach to the released DNA1. Compared to **curve b**, MB oxidation peak current in **curve c** significantly increased, which resulted in the formation of complex DNA structure (Fig. 1A c and Fig. 1B, **curve c**). These results indicated the feasibility of our NE-based dual-signal ratiometric biosensor for GSH detection.

3.3. Optimization of the $AgNO_3$ concentration

Since GSH has a strong affinity for silver nanoparticles, we optimized the concentration of silver nitrate solution to obtain the optimum silver nanoparticles. Fig. 2A showed the DPV curves of DNA1/NEs modified by different concentrations of $AgNO_3$ solution (100 μM, 200 μM, 400 μM, 600 μM, 800 μM, 1000 μM, 1200 μM). As the $AgNO_3$ concentration increases, the oxidation peak current of Ag also increases, when the concentration reaches 1000 μM the peak current changes tend to be stable (Fig. 2B). Therefore, 1000 μM was chosen as the optimal concentration of $AgNO_3$. To further demonstrate that silver nanoparticles were successfully synthesized, TEM characterization was performed in Fig. S2A. The size distribution of prepared Ag nanoparticles was shown in Fig. S2B. The average size of the silver nanoparticles is about 6 nm.

3.4. Electrochemical detection of GSH

The DPV curves of MB and Ag at the MB/Ag/DNA1/NEs in different concentrations of GSH were shown in Fig. 3A. As the concentration of GSH increases, the peak current of MB increases, and the oxidation current of Ag decreases. To amplify the electrochemical response, the current ratio of "I_{MB}/I_{Ag}" is used for the quantitative determination of the concentration of GSH. From 10 nM to 800 nM, with the concentration of GSH increases, the current ratio value also increases linearly. The linear function could be express as: $I_{MB}/I_{Ag} = 0.0762 + 0.0036\ C_{GSH}$ (nM) ($R^2 = 0.9948$, Fig. 3B). The limit of detection (LOD) was calculated to be 0.7 nM based on the equation of LOD = 3 S_b/m reported in Refs. [38,39] To compare the analytical performance of our dual-signaling sensors and reported single-signaling sensors for GSH detection, a linear fit was made to ΔI_{Ag} and C_{GSH} in Fig. S3. A linear relationship between I_{Ag} and GSH concentration was obtained in the range of 20 nM−200 nM. Compared with non-proportional sensors, our NEs-based biosensor has a wider linear range and comparable detection limits. The LOD value obtained by this method is much lower than most other detection methods (Table 1). It should be noticed that our dual-signaling sensors can still work normally in the high concentration range (Fig. S4).

3.5. Selectivity and reproducibility of the electrochemical biosensor

To investigate the specific response of the dual-signaling ratiometric amplification electrochemical biosensor to GSH, the values of I_{MB}/I_{Ag} were obtained in the solution containing different amino acids. The result was shown in Fig. 4A. These results indicate that the responses to amino acids other than Cys and GSH are almost negligible, which is mainly due to the high binding affinity between the thiol and Ag NP through the formation of Ag−S bonds. But the concentration of Cys (micromolar levels) is remarkably lower than the concentration of GSH (millimolar levels) in mammalian cells [18,24]. Thus, this strategy could be used for selectively detecting GSH in a living system.

To further demonstrate that the biosensor has good reproducibility for GSH, five parallel experiments were carried out (Fig. 4B, RSD = 1.2%). Our dual-signaling sensors show good stability to the detection of GSH.

3.6. GSH detection in real samples

To evaluate the performance of the prepared sensors in a biological environment, the study was carried out in HeLa cell lysate. In mammalian cells, Cys concentration is much lower than the GSH concentration [40], so that Cys cannot interfere with the detection of GSH. The diluted cell lysate samples were spiked with three different concentrations of GSH (Table 2). These satisfactory recovery rates (96.52%−101.64% in HeLa cell lysate) indicate that the method can be used to measure GSH in biological systems, and the results can reflect the biological state to a certain extent.

4. Conclusions

In summary, a nanoelectrodes-based dual-signaling ratiometric amplification biosensor using Ag nanoparticles and MB as signals has been developed. With the addition of GSH, due to the strong affiant binding between GSH and Ag NPs, DNA1 could be released and further hybrid to form a complex structure to attach MB. This will decrease the Ag oxidation current and increase the MB signal. These NEs-based sensors are simple and label-free. Adopting the ratiometric dual-signal strategy can avoid intrinsic systematic errors, enabling the assay to be more sensitive. Considering the nm-level size of the sensors, we believe that our new NEs-based sensors will have promising applications in the detection of GSH in the living systems with high sensitivity and selectivity.

CRediT authorship contribution statement

Hao Wang: Conceptualization, Methodology, Data curation, Writing − original draft. **Hongmei Hua:** Data curation, Writing − original draft. **Haoran Tang:** Methodology, Investigation. **Yongxin Li:** Conceptualization, Writing − review & editing, Supervision, Funding acquisition.

Declaration of competing interest

The authors declare that they have no known competing

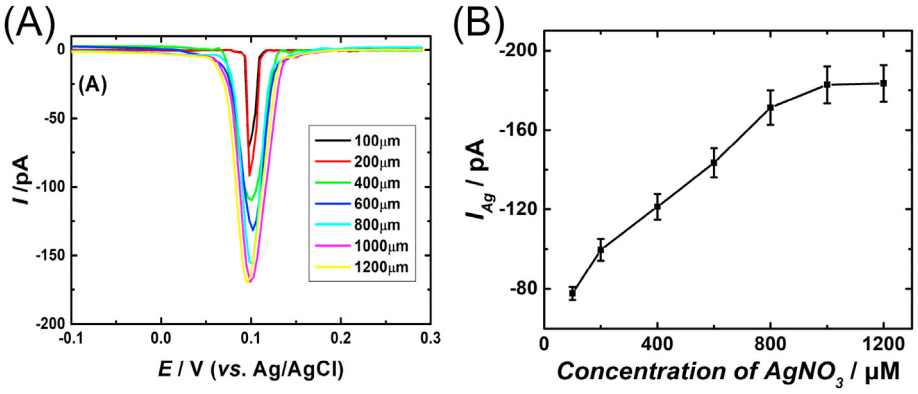

Fig. 2. **(A)** DPV curves of the different $AgNO_3$ concentrations in the Ag/DNA1/NE. **(B)** $AgNO_3$ concentration optimizes dot plot.

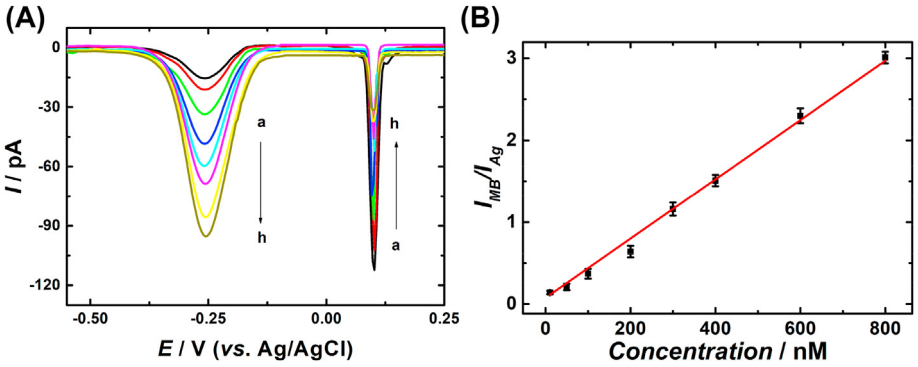

Fig. 3. **(A)** DPV curves of the MB/DNA1/Ag/NEs for detection of different concentrations of GSH. The concentrations are (from **a** to **h**) 10 nM, 50 nM, 100 nM, 200 nM, 300 nM, 400 nM, 600 nM, 800 nM. **(B)** The linear fit plot of I_{MB}/I_{Ag} and GSH. Error bars were estimated from at least three independent measurements. The diameter of the Au nanodisk electrode was about 126 nm.

Table 1
Comparison of different methods for GSH sensing.

methods	probes	Linear range	LOD	ref
fluorescence	BODIPY derivatives	0–60 μM	86 nM	[10]
fluorescence	MnO_2-CQDs nanocomposites	0–250 μM	300 nM	[18]
colorimetry	Naphthalimide-capped AuNPs	0.025–2.28 μM	17 nM	[41]
HPLC	Nonionic surfactant-capped Gold nanoparticles		2.0 μM	[42]
SERS	γ-Fe_2O_3–Au	1 pM-10 μM	1pM	[43]
ECL	Core-shell CdSe/ZnS quanturn dots/Nafion composite film	10–180 μM	1.57 μM	[44]
electrochemistry	DNA metallization chain composite Au nanodisk electrode	10–800 nM	0.7 nM	This work

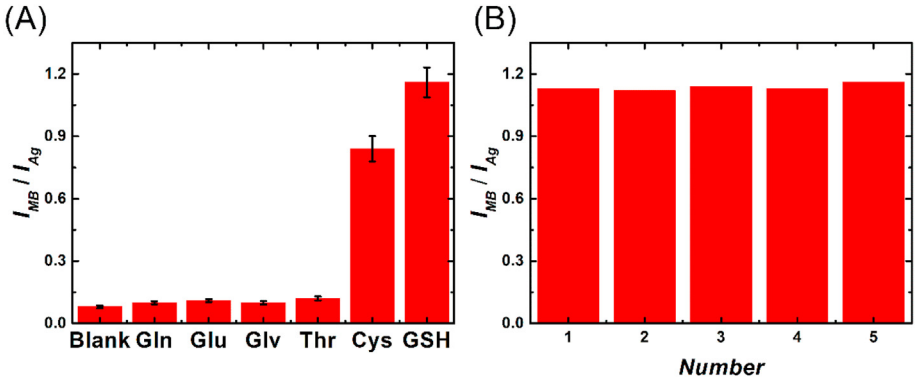

Fig. 4. **(A)** The ratio I_{MB}/I_{Ag} of the probe in the presence of different amino acids. The concentrations of amino acids were 400 nM. The radius of Au nanodisk electrodes was 129 nm. **(B)** The reproducibility of the dual-signaling ratiometric amplification electrochemical biosensor. The radius of Au nanodisk electrodes was 127 nm. RSD = 1.2%.

Table 2
GSH detection in real Samples.

Samples	Found in the sample (nM)	Spiked (nM)	Total found (nM)	RSD (%, n = 3)	Recovery (%, n = 3)
HeLa cell lysate		100.00	315.96	2.28	96.52
	227.35	200.00	434.35	1.94	101.64
		300.00	515.45	2.69	97.74

financial interests or personal relationships that could have appeared to influence the work reported in this paper.

Acknowledgments

This work is financially supported by the National Natural Science Foundation of China (No.21775003, No.21375002), the Foundation for Innovation Team of Bioanalytical Chemistry of Anhui Province.

Appendix A. Supplementary data

Supplementary data to this article can be found online at https://doi.org/10.1016/j.aca.2021.338579.

References

[1] S.C. Lu, Regulation of glutathione synthesis, Mol. Aspect. Med. 30 (2009) 42–59.
[2] A. Meister, M.E. Anderson, Glutathione, Annu. Rev. Biochem. 52 (1983) 711–760.
[3] J. Richie Jr., L. Skowronski, P. Abraham, Y. Leutzinger, Blood glutathione concentrations in a large-scale human study, Clin. Chem. 42 (1996) 64–70.
[4] S. Singh, J. Wishnok, M. Keshive, W. Deen, S. Tannenbaum, The chemistry of the S-nitrosoglutathione/glutathione system, P. Natl. Acad. Sci. 93 (1996) 14428–14433.
[5] B. Halliwell, Antioxidants in human health and disease, Annu. Rev. Nutr. 16 (1996) 33–50.
[6] K. Ngamchuea, C. Batchelor-McAuley, R.G. Compton, Rapid method for the quantification of reduced and oxidized glutathione in human plasma and saliva, Anal. Chem. 89 (2017) 2901–2908.
[7] Y. Gao, K. Wu, H. Li, W. Chen, M. Fu, K. Yue, et al., Glutathione detection based on peroxidase-like activity of Co3O4–Montmorillonite nanocomposites, Sensor. Actuator. B Chem. 273 (2018) 1635–1639.
[8] X.-L. Fu, F. Hou, F.-R. Liu, S.-W. Ren, J.-T. Cao, Y.-M. Liu, Electrochemiluminescence energy resonance transfer in 2D/2D heterostructured g-C3N4/MnO2 for glutathione detection, Biosens. Bioelectron. 129 (2019) 72–78.
[9] L. Dennany, M. Gerlach, S. O'Carroll, T.E. Keyes, R.J. Forster, P. Bertoncello, Electrochemiluminescence (ECL) sensing properties of water soluble core-shell CdSe/ZnS quantum dots/Nafion composite films, J. Mater. Chem. 21 (2011) 13984–13990.
[10] W. Gao, Z. Liu, L. Qi, J. Lai, S.A. Kitte, G. Xu, Ultrasensitive glutathione detection based on lucigenin cathodic electrochemiluminescence in the presence of MnO2 nanosheets, Anal. Chem. 88 (2016) 7654–7659.
[11] A. Saha, N.R. Jana, Detection of cellular glutathione and oxidized glutathione using magnetic–plasmonic nanocomposite-based "Turn-Off" surface enhanced Raman scattering, Anal. Chem. 85 (2013) 9221–9228.
[12] R. Deng, X. Xie, M. Vendrell, Y.-T. Chang, X. Liu, Intracellular glutathione detection using MnO2-nanosheet-modified upconversion nanoparticles, J. Am. Chem. Soc. 133 (2011) 20168–20171.
[13] G. Garai-Ibabe, L. Saa, V. Pavlov, Enzymatic product-mediated stabilization of CdS quantum dots produced in situ: application for detection of reduced glutathione, NADPH, and glutathione reductase activity, Anal. Chem. 85 (2013) 5542–5546.
[14] D. He, X. Yang, X. He, K. Wang, X. Yang, X. He, et al., A sensitive turn-on fluorescent probe for intracellular imaging of glutathione using single-layer MnO 2 nanosheet-quenched fluorescent carbon quantum dots, Chem. Commun. 51 (2015) 14764–14767.
[15] L.-Y. Niu, Y.-S. Guan, Y.-Z. Chen, L.-Z. Wu, C.-H. Tung, Q.-Z. Yang, BODIPY-based ratiometric fluorescent sensor for highly selective detection of glutathione over cysteine and homocysteine, J. Am. Chem. Soc. 134 (2012) 18928–18931.
[16] Q.-Y. Cai, J. Li, J. Ge, L. Zhang, Y.-L. Hu, Z.-H. Li, et al., A rapid fluorescence "switch-on" assay for glutathione detection by using carbon dots–MnO2 nanocomposites, Biosens. Bioelectron. 72 (2015) 31–36.
[17] H. Xu, Y. Wang, X. Huang, Y. Li, H. Zhang, X. Zhong, Hg 2+-mediated aggregation of gold nanoparticles for colorimetric screening of biothiols, Analyst 137 (2012) 924–931.
[18] C. Lu, Y. Zu, V.W.-W. Yam, Nonionic surfactant-capped gold nanoparticles as postcolumn reagents for high-performance liquid chromatography assay of low-molecular-mass biothiols, J. Chromatogr. A 1163 (2007) 328–332.
[19] Y.H. Shao, M.V. Mirkin, G. Fish, S. Kokotov, D. Palanker, A. Lewis, Nanometer-sized electrochemical sensors, Anal. Chem. 69 (1997) 1627–1634.
[20] P. Sun, M.V. Mirkin, Kinetics of electron-transfer reactions at nanoelectrodes, Anal. Chem. 78 (2006) 6526–6534.
[21] B. Zhang, Y.H. Zhang, H.S. White, The nanopore electrode, Anal. Chem. 76 (2004) 6229–6238.
[22] B. Zhang, Y.H. Zhang, H.S. White, Steady-state voltammetric response of the nanopore electrode, Anal. Chem. 78 (2006) 477–483.
[23] Y. Li, D. Bergman, B. Zhang, Preparation and electrochemical response of 1-3 nm Pt disk electrodes, Anal. Chem. 81 (2009) 5496–5502.
[24] B.B. Katemann, W. Schuhmann, Fabrication and characterization of needle-type Pt-disk nanoelectrodes, Electroanalysis 14 (2002) 22–28.
[25] T. Wang, E. Viennois, D. Merlin, G. Wang, Microelectrode miRNA sensors enabled by enzyme less electrochemical signal amplification, Anal. Chem. 87 (2015) 8173–8180.
[26] P. Actis, S. Tokar, J. Clausmeyer, B. Babakinejad, S. Mikhaleva, R. Cornut, et al., Electrochemical nanoprobes for single-cell analysis, ACS Nano 8 (2014) 875–884.
[27] B.K. Jena, S.J. Percival, B. Zhang, Au disk nanoelectrode by electrochemical deposition in a nanopore, Anal. Chem. 82 (2010) 6737–6743.
[28] S.E. Salamifar, R.Y. Lai, Fabrication of electrochemical DNA sensors on gold-modified recessed platinum nanoelectrodes, Anal. Chem. 86 (2014) 2849–2852.
[29] M. Marquitan, J. Clausmeyer, P. Actis, A.L. Cordoba, Y. Korchev, M.D. Mark, et al., Intracellular hydrogen peroxide detection with functionalised nanoelectrodes, Chemelectrochem 3 (2016) 2125–2129.
[30] Y. Wang, J.-M. Noel, J. Velmurugan, W. Nogala, M.V. Mirkin, C. Lu, et al., Nanoelectrodes for determination of reactive oxygen and nitrogen species inside murine macrophages, P. Natl. Acad. Sci. USA 109 (2012) 11534–11539.
[31] Y. Li, K. Hu, Y. Yu, S.A. Rotenberg, C. Amatore, M.V. Mirkin, Direct electrochemical measurements of reactive oxygen and nitrogen species in non-transformed and metastatic human breast cells, J. Am. Chem. Soc. 139 (2017) 13055–13062.
[32] D. Wang, X. Xiao, S. Xu, Y. Liu, Y. Li, Electrochemical aptamer-based nanosensor fabricated on single Au nanowire electrodes for adenosine triphosphate assay, Biosens. Bioelectron. 99 (2018) 431–437.
[33] H. Tang, J. Zhu, D. Wang, Y. Li, Dual-signal amplification strategy for miRNA sensing with high sensitivity and selectivity by use of single Au nanowire electrodes, Biosens. Bioelectron. 131 (2019) 88–94.
[34] D. Wang, H. Hua, H. Tang, C. Yang, W. Chen, Y. Li, A signal amplification strategy and sensing application using single gold nanoelectrodes, Analyst 144 (2019) 310–316.
[35] Y. Zhang, S. Xu, X. Xiao, Y. Liu, Y. Qian, Y. Li, Single gold nanowire electrodes and single Pt@ Au nanowire electrodes: electrochemistry and applications, Chem. Commun. 53 (2017) 2850–2853.
[36] D. Zhao, H. Tang, H. Wang, C. Yang, Y. Li, Analytes triggered conformational switch of i-motif DNA inside gold-decorated solid-state nanopores, ACS Sens. 5 (2020) 2177–2183.
[37] A.J. Bard, L.R. Faulkner, Electrochemical Methods, John Wiley & Sons, New York, 2001.
[38] Q. Feng, M. Wang, X. Han, Q. Chen, B. Dou, P. Wang, Construction of an electrochemical biosensing platform based on hierarchical mesoporous NiO@ N-doped C microspheres coupled with catalytic hairpin assembly, ACS Applied Bio Materials 3 (2020) 1276–1282.
[39] Q. Chen, T. Tian, E. Xiong, P. Wang, X. Zhou, CRISPR/Cas13a signal amplification linked immunosorbent assay for femtomolar protein detection, Anal. Chem. 92 (2019) 573–577.
[40] J. Liu, Y.-Q. Sun, Y. Huo, H. Zhang, L. Wang, P. Zhang, et al., Simultaneous fluorescence sensing of Cys and GSH from different emission channels, J. Am. Chem. Soc. 136 (2014) 574–577.
[41] N.F. Atta, A. Galal, S.M. Azab, Novel sensor based on carbon paste/Nafion® modified with gold nanoparticles for the determination of glutathione, Anal. Bioanal. Chem. 404 (2012) 1661–1672.
[42] L. Berti, A. Alessandrini, P. Facci, DNA-templated photoinduced silver deposition, J. Am. Chem. Soc. 127 (2005) 11216–11217.
[43] J.C. Harfield, C. Batchelor-McAuley, R.G. Compton, Electrochemical determination of glutathione: a review, Analyst 137 (2012) 2285–2296.
[44] H.R.L.Z. Zhad, R.Y. Lai, A Hg (II)-mediated "signal-on" electrochemical glutathione sensor, Chem. Commun. 50 (2014) 8385–8387.